EAST EUROPEAN JOURNAL OF PHYSICS. 1. 75-81 (2023)
DOI:10.26565/2312-4334-2023-1-08 ISSN 2312-4334

THEORETICAL STUDY OF PROTON HALO STRUCTURE AND ELASTIC ELECTRON SCATTERING FORM FACTOR FOR ^{23}Al AND ^{27}P NUCLEI BY USING FULL CORRELATION FUNCTIONS (TENSOR FORCE AND SHORT RANGE)[†]

Abeer A.M. Hussein*, Ghaith N. Flaiyh
Department of Physics, College of Science, University of Baghdad, Baghdad, Iraq
**Corresponding Author e- mail: Abeer.Ali1104a@sc.uobaghdad.edu.iq*
Received November 13, 2022; revised December 12, 2022; accepted December 15, 2022

The study of proton-rich nuclei's form factors, root-mean-square radius (*rms*), and nuclear density distributions is the focus of this work for nuclei (^{23}Al and ^{27}P), use two body charge density distributions (2BCDD's). With the effects of the strong tensor force and short range, the nucleon distribution function of the two oscillating harmonic particles in a two-frequency shell model operates with two different parameters: bc for the inner (core) orbits and bv for the outer (halo) orbitals. This work demonstrated the existence of proton halo nuclei for the nuclei (^{23}Al and ^{27}P) in the shell ($2s_{1/2}$), and the computed proton, neutron, and matter density distributions for these nuclei both displayed the long tail of the performance. Using the Borne approximation of the plane wave, the elastic form factor of the electron scattering from the alien nucleus was calculated, this form factor is dependent on the difference in the proton density distribution of the last proton in the nucleus. The Fortran 95 power station program was used to calculate the neutrons, protons, matter density, elastic electron scattering form factor, and *rms* radii. The calculated outcomes for these exotic nuclei agree well with the experimental data.
Keywords: *Exotic nuclei; Form Factor; Proton-rich; Root mean square (rms) radii*
PACS: 21.10.Ft, 21.10.Gv, 21.45.Bc, 21.60.n, 21.65.f

1. INTRODUCTION

The nuclear halo is a threshold effect with low separation energy. There are two different kinds of exotic halo nuclei: proton halo [1] and neutron halo [2,3]. Neutron halo nuclei have recently undergone extensive experimental and theoretical study [4,5]. However, studies on proton halos are very rare. Although the proton separation energy in some light nuclei such as ^{8}B and ^{17}F is very low [4,6-7].

Emil Ryberg and others examined the impact of finite-range corrections for S-wave proton halo nuclei on the halo effective field theory [8]. Dellagiacoma et al. [9] provided a straightforward phenomenological technique for creating dynamical short-range and tensor correlations. Da Providencia and Shakin [10] developed a similar correlation operator for explaining short-range correlation effects, as did Malecki and Picchi [11]. Luay F. Sultan [12] used the binary cluster model within the single-particle wave functions of Gaussian and harmonic oscillator potentials to investigate the ground state density distributions of proton-rich ^{23}Al and ^{27}P halo nuclei. The radial wave functions of the calculated Woods–Saxon potentials for ^{8}B, ^{17}F, 17Ne, ^{23}Al, and ^{27}P have been used before Rafah I. Noori [13].

Using a coherent density fluctuation model and 2pF to study one- and two-proton halo nuclei for ^{23}Al, ^{26}P, and ^{28}S nuclei is presented by Maha Taha Yassin [14]. The two-frequency shell model and the binary cluster model are used to investigate the ground state densities of unstable proton-rich ^{9}C, ^{12}N, and ^{23}Al exotic nuclei [15].

In this study, we will use the two-body charge density distributions (2BCDD's) in the ground state for the proton-rich nuclei for (^{23}Al and ^{27}P) with full correlations (tensor force and short range) with we used two different oscillator size parameters bc and bv and we calculated of rms radii, density distributions for (protons, neutrons, and matter) and form factors for these exotic nuclei.

2. THEORY

The operator has been used to define the nucleon density of a point-like particle nucleus [16]:

$$\hat{\rho}^{(1)}(\vec{r}) = \sum_{i=1}^{A} \delta\left(\vec{r} - \vec{r}_i\right). \tag{1}$$

This operator can be transformed into a two- body density form ($\hat{\rho}^{(1)}(\vec{r}) \Rightarrow \hat{\rho}^{(2)}(\vec{r})$) as [17]:

$$\sum_{i=1}^{A} \delta\left(\vec{r} - \vec{r}_i\right) \equiv \frac{1}{2(A-1)} \sum_{i \neq j} \left\{ \delta\left(\vec{r} - \vec{r}_i\right) + \delta\left(\vec{r} - \vec{r}_i\right) \right\}. \tag{2}$$

Another relevant transformation is that of the coordinates of the two particles, which may be expressed, ($\vec{r}_i$ and $\vec{r}_j$) in terms -of- that relative $\vec{r}_{ij}$ and center -of- mass $\vec{R}_{ij}$ coordinates [18]:

[†] ***Cite as:*** A.A.M. Hussein, and G.N. Flaiyh, East Eur. J. Phys. **1**, 82 (2023), https://doi.org/10.26565/2312-4334-2023-1-08

$$\vec{r}_{ij} = \frac{1}{\sqrt{2}}\left(\vec{r}_i - \vec{r}_j\right), \tag{3-a}$$

$$\vec{R}_{ij} = \frac{1}{\sqrt{2}}(\vec{r}_i + \vec{r}_j), \tag{3-b}$$

Subtracting and adding (3-a) and (3-b) can be obtain:

$$\vec{r}_i = \frac{1}{\sqrt{2}}(\vec{R}_{ij} + \vec{r}_{ij}), \tag{3-c}$$

$$\vec{r}_j = \frac{1}{\sqrt{2}}(\vec{R}_{ij} - \vec{r}_{ij}). \tag{3-d}$$

Using eqs. (3-c) and (3-d) in Eq (2), we obtain:

$$\hat{\rho}^{(2)}(\vec{r}) = \frac{1}{2(A-1)}\sum_{i\neq j}\left\{\delta\left[\vec{r} - \frac{1}{\sqrt{2}}(\vec{R}_{ij} + \vec{r}_{ij})\right] + \delta\left[\vec{r} - \frac{1}{\sqrt{2}}(\vec{R}_{ij} - \vec{r}_{ij})\right]\right\} \tag{4}$$

Using the identity $\delta(a\vec{r}) = \frac{1}{|a^3|}\delta(\vec{r})$ (for three –dimension), where (a) is a constant. For closed shell nuclei with N=Z, the two–body charge density operator can be deduced from Eq. (4) as:

$$\hat{\rho}^{(2)}_{ch}(\vec{r}) = \frac{1}{2}\hat{\rho}^{(2)}(\vec{r})$$

i.e.

$$\hat{\rho}^{(2)}_{ch}(\vec{r}) = \frac{\sqrt{2}}{(A-1)}\sum_{i\neq j}\left\{\delta\left[\sqrt{2}\vec{r} - \vec{R}_{ij} - \vec{r}_{ij}\right] + \delta\left[\sqrt{2}\vec{r} - \vec{R}_{ij} + \vec{r}_{ij}\right]\right\}. \tag{5}$$

The operator from Equation (5) can be folded with the two–body correlation functions $\tilde{f}_{ij}$ to yield an efficient two–body charge density operator.

$$\hat{\rho}^{(2)}_{eff}(\vec{r}) = \frac{\sqrt{2}}{(A-1)}\sum_{i\neq j}\tilde{f}_{ij}\left\{\delta\left[\sqrt{2}\vec{r} - \vec{R}_{ij} - \vec{r}_{ij}\right] + \delta\left[\sqrt{2}\vec{r} - \vec{R}_{ij} + \vec{r}_{ij}\right]\right\}\tilde{f}_{ij}, \tag{6}$$

where the from $\tilde{f}_{ij}$ is given by [18]

$$\tilde{f}_{ij} = f(r_{ij})\Delta_1 + f(r_{ij})\left\{1 + \alpha(\mathrm{A})P_{ij}\right\}\Delta_2. \tag{7}$$

It is clear that eq. (7) contains two kinds of correlations:

- The first term of equation (7)'s two–body short range correlations, which is expressed as $f(\mathrm{r_{ij}})$. Here Δ_1 With the exception of $^3\mathrm{S}_1$ and $^3\mathrm{D}_1$ states, is a projection operator onto the space of all two–body wave functions. Short-range correlations should be observed as important functions of particle separation, which diminish the two-body wave function at short distances where the repulsive core forces the particles apart and heal to unity at a lengthy distance where the interactions are very weak. The two–body short-range correlation is given by [18]:
- $$f(r_{ij}) = \begin{Bmatrix} 0 & for\ r_{ij} \le r_c \\ 1 - \exp\left\{-\mu(r_{ij} - r_c)^2\right\} & for\ r_{ij} > r_c \end{Bmatrix} \tag{8}$$

where r_c (fm) is the radius of a suitable hard core and, $\mu = 25\ fm^{-2}$ [20] correlation parameter.

- The strong tensor component in the nucleon-nucleon force induces the longer range two body tensor correlations that are shown in the second term of equation (7).

$$\tilde{f}_{ij} = f(r_{ij})\left\{1 + \alpha(\mathrm{A})P_{ij}\right\}\Delta_2, \tag{9}$$

into triplet $^3S_1 - {}^3D_1$ channels, where

$$\Delta_2 = \sum_{\ell SgT}\left|(\ell S)gT\right\rangle\left\langle(\ell S)gT\right|. \tag{10}$$

This projection operator only affects the $^3S_1$ and $^3D_1$ states. The typical tensor operator, P_{ij}, is known as [18]:

$$P_{ij} = \frac{3}{r_{ij}^2}\left(\vec{\sigma}_i \cdot \vec{r}_{ij}\right)\left(\vec{\sigma}_j \cdot \vec{r}_{ij}\right) - \vec{\sigma}_i.\vec{\sigma}_j . \tag{11}$$

While α (A) can be defined as the strength of tensor correlation and it is non-zero just in the $^3S_1$ and $^3D_1$ channel. Where the relative orbital angular momentum (ℓ) and total spin (S) of two particles are coupled to the channel spin (g) a projection operator onto triplet coupled states of $^3S_1$ and $^3D_1$. In Eq. (7) the radial part is easily included as it only modifies the radial integrals involving r_{12}. Acting the operator of Eq. (6) into triplet $^3S_1$ state

$$\tilde{f}_{12}\left|{}^3S_1\right\rangle = f(r_{12})\left\{\ 1+\alpha(\mathrm{A})\,P_{12}\ \right\}\left|{}^3S_1\right\rangle\Delta_2 , \tag{12}$$

and acting the operator $\tilde{f}_{12}$ into triplet $^3D_1$, we get

$$\tilde{f}_{12}\left|{}^3D_1\right\rangle = f(r_{12})\left\{\ 1+\alpha(\mathrm{A})\,P_{12}\ \right\}\left|{}^3D_1\right\rangle\Delta_2 . \tag{13}$$

It makes sense to parameterize the core and halo densities independently in the case of exotic nuclei. Consequently, the following is how the halo nuclei's ground-state matter density distribution can be expressed [19]:

$$\rho_m(r) = \rho^{core}_{(p+n)}(r) + \rho^{valence}_n(r) . \tag{14}$$

The normalization condition of the above ground state densities is given by:

$$g = 4\pi\int_0^\infty \rho^g(r) r^2 dr , \tag{15}$$

here $\rho^g(\mathrm{r})$ represents one of the following densities: nucleon, charge, core, halo densities. The *rms* radii of corresponding above densities are given by [20]:

$$\left\langle r^2\right\rangle_g^{1/2} = \frac{4\pi}{g}\int_0^\infty \rho^g(r) r^4 dr , \tag{16}$$

where g is (proton, neutron or matter).

The PWBA was used to study the elastic electron scattering form factors from emitted by the nuclei under study. The charge form factor in PWBA is [21]:

$$F(q) = \frac{4\pi}{qZ}\int_0^\infty \rho_o(\mathrm{r})\,\mathrm{Sin}(q\mathrm{r})\,\mathrm{r}\ d\mathrm{r}\, F_{fs}(q)\, F_{cm}(q) , \tag{17}$$

where the nucleon finite size correction F_{fs} *(q)* is defined [22]:

$$F_{fs}(q) = e^{-0.43q^2/4} , \tag{18}$$

where the free nucleon form factor F_{fs} (q) for protons and neutrons is consider to be the same. According to [23], the center of mass correction F_{cm} *(q)* is as follows:

$$F_{cm}(q) = e^{q^2b^2/4A} , \tag{19}$$

where b : The harmonic-oscillator size parameter and A : The nuclear mass number.

As a result, when the shell model wave function is, removes F_{cm} *(q)* eliminates the spurious state caused by the center of mass's motion. The form factor *F(q)* comprising the impact of two-body correlation functions may now be calculated by entering the ground state *(r)* of equation (6) into equation (14).

3. RESULTS AND DISCUSSION

The density distributions for (protons, neutrons, and matter) of the ground state of (^{23}Al and ^{27}P) nuclei and *rms* radii with the form factors *F(q)* were studied by the two body charge density distributions (2BCDD's) with effect short-range and tensor force by using the two body oscillator model (core +1p) shell model with used parameters (bc), (bv), and by relying on equations 6, 7, and 11.

Table 1, summarizes some of the characteristics of halo nuclei [24,25]. The average radius of neutrons and protons was calculated based on equations 6, 7, and 16, where we got the results shown in Table 2, when the full correlation (r_c=0.5 *fm*, α =0.1) and without correlation (r_c=0, α=0). It is found that the proton *rms* radius is larger than the neutron *rms* radius.

Table 1. Some properties of ^{23}Al and ^{27}P nuclei

Exotic nucleus	J^{Π}, T [25]	Nuclei core	J^{Π}, T [25]	Half life time ($T_{1/2}$) [24]	Separation energy (*Mev*)[24]
^{23}Al	1/2$^+$,3/2	^{22}Mg	0$^+$, 1	470 ms	0.141
^{27}P	1/2$^+$,3/2	^{26}Si	0$^+$, 1	260 ms	0.870

Table 2. The calculated neutrons and protons *rms* radii for nuclei (^{23}Al and ^{27}P)

Exotic nuclei ^{23}Al			
Proton size parameter	b_p=2 *fm*	Neutron size parameter	b_n=1.75 *fm*
$\langle r_p^2\rangle^{1/2}_{r_c=0.5,\alpha=0.1}$	3.195974	$\langle r_n^2\rangle^{1/2}_{r_c=0.5,\alpha=0.1}$	2.669840
$\langle r_p^2\rangle^{1/2}_{r_c=0,\alpha=0}$	3.203143	$\langle r_n^2\rangle^{1/2}_{r_c=0,\alpha=0}$	2.667579
$\langle r_p^2\rangle^{1/2}_{exp}$ [25]	3.1 ± 0.25	$\langle r_n^2\rangle^{1/2}_{exp}$ [25]	2.634 ± 0.23
$\langle r_p^2\rangle^{1/2}_{FC's}$	-0.0071	$\langle r_n^2\rangle^{1/2}_{FC's}$	-0.0022
Exotic nuclei ^{27}P			
Proton size parameter	b_p=2.05 *fm*	Neutron size parameter	b_n=1.73*fm*
$\langle r_p^2\rangle^{1/2}_{r_c=0.5,\alpha=0.1}$	3.395257	$\langle r_n^2\rangle^{1/2}_{r_c=0.5,\alpha=0.1}$	2.744588
$\langle r_p^2\rangle^{1/2}_{r_c=0,\alpha=0}$	3.405219	$\langle r_n^2\rangle^{1/2}_{r_c=0,\alpha=0}$	2.745390
$\langle r_p^2\rangle^{1/2}_{exp}$ [25]	3.22 ± 0.163	$\langle r_n^2\rangle^{1/2}_{exp}$ [25]	2.754 ± 0.14
$\langle r_p^2\rangle^{1/2}_{FC's}$	-0.0099	$\langle r_n^2\rangle^{1/2}_{FC's}$	-0.0008

Table 3, shows the calculated *rms* radii for core nuclei (^{22}Mg and ^{26}Si) with oscillator size parameter (b_c =2.85, 187) for ^{22}Mg and ^{26}Si respectively, and exotic nuclei (^{23}Al and ^{27}P) with oscillator size parameter (b_m =1.87, 2.015) for^{23}Al and ^{27}P respectively with effects of the short-range (r_c= 0.5 *fm*) and the tensor force (α= 0.1).

Table 3. The calculated core, valance and matter radii *rms* with experimental data for ^{23}Al and ^{27}P nuclei

Halo nuclei	Core nuclei	b_c	b_v	b_m	***rms* matter radii for core nuclei $\langle r^2\rangle_c^{1/2}$ (*fm*)**		***rms* matter radii for halo nuclei $\langle r^2\rangle_h^{1/2}$ (*fm*)**	
					Calculated results	Experimental Data	Calculated results	Experimental Data
^{23}Al	^{22}Mg	1.85	3.85	1.87	2.872617	2.78 ± 0.26 [26]	2.911843	2.905 ± 0.25 [26]
^{27}P	^{26}Si	1.87	3.5	1.912	3.025680	2.88 ± 0.06 [27]	3.028345	3.02 ± 0.155 [27]

The calculated results are in good agreement with the indicated experimental data [26,27]. The correlation short range force with root mean square radii $\langle r^2\rangle^{1/2}$. We note an increase in *rms* values with an increase in short-range force by relying on equations (7, 8), as we showed in Table 4. Table 5, show correlation tensor force with *rms* radii $\langle r^2\rangle^{1/2}$. It is found to decrease *rms* values with increased tensor force by relying on equations (7, 9), and 11.

Table 4. The calculated of the *rms* radii with different values for the short-range correlations for ^{23}Al and ^{27}P nuclei

r_c (*fm*)	$\langle r^2\rangle^{1/2}$ for ^{23}AL nuclei	$\langle r^2\rangle^{1/2}$ for ^{27}P nuclei
0.3	2.898914	3.01684
0.35	2.899032	3.016960
0.4	2.900136	3.017976
0.45	2.903780	3.021325
0.5	2.911843	3.028711
0.55	2.923239	3.039108

Table 5. The calculated of the *rms* radii with different values for the tensor force correlations for ^{23}Al and ^{27}P nuclei

α	$\langle r^2 \rangle^{1/2}$ for ^{23}AL nuclei	$\langle r^2 \rangle^{1/2}$ for ^{27}P nuclei
0.07	2.916419	3.032756
0.075	2.915664	3.032097
0.08	2.914908	3.031432
0.085	2.914147	3.030761
0.09	2.913382	3.030083
0.095	2.912615	3.029400
0.1	2.911843	3.028711

Figure 1 shows the relation between the two-body nucleon density distributions (2BNDD's) (in fm^{-3}) of the ground state and r (in *fm*) for ^{23}Al and ^{27}P nuclei. The blue curve represents 2BNDD's for the core nuclei ^{22}Mg and ^{26}Si (proton + neutron) with oscillator size parameter (bc =2.85, 187) respectively. The green curve represents 2BNDD's for valence (one proton) for ^{23}Al and 27P nuclei with oscillator size parameter (bv=3.85, 3.5) respectively, while the red solid curve represents the total calculation for the core nucleons and the valence one proton, and the shaded curve represents the experimental of nucleon densities of ^{23}Al and ^{27}P respectively [25,26]. Figure 1 shows that the computed matter density distributions show a long tail for all of these nuclei and shows that the halo phenomenon and the long tail in ^{23}Al and ^{27}P are connected to the outer one proton for nucleon densities but not to the core nucleons, which is consistent with the experimental data.

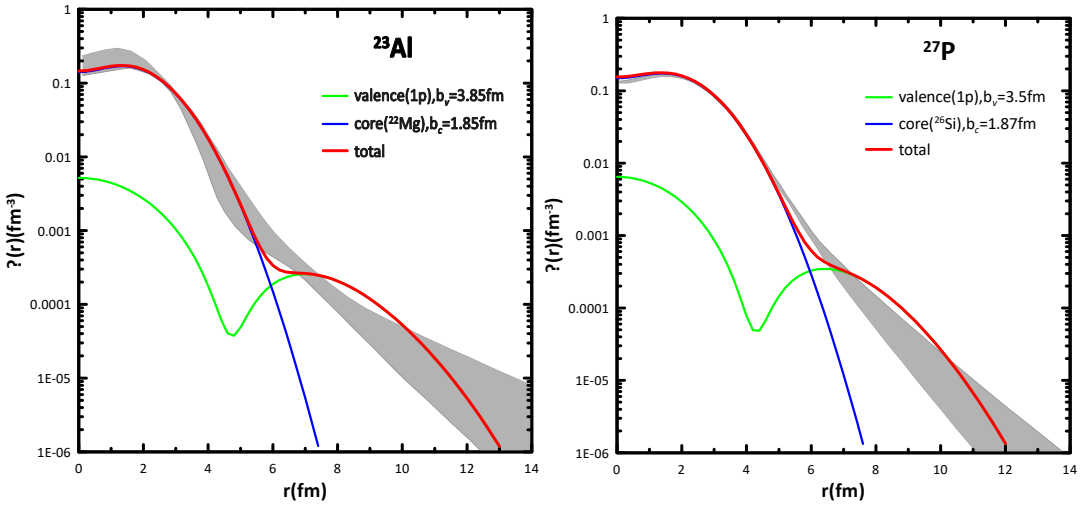

Figure 1. Core, halo and matter density distribution of (^{23}Al and ^{27}P).

Figure 2 illustrates a comparison of the matter density distributions of halo (^{23}Al and ^{27}P) (red line) with the matter density distributions of the stable nuclei (^{27}Al and ^{31}P) (yellow line) by using 2BCDD's with the effect of short-range and tensor force, we shown along tail is clearly in the matter distribution of the halo nuclei.

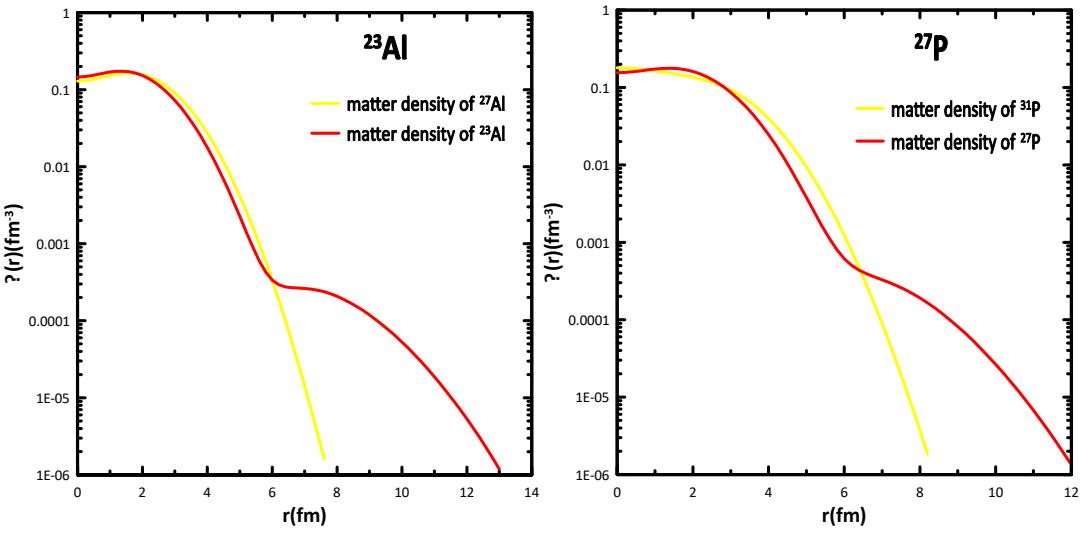

Figure 2. Comparison of matter density distribution of exotic nuclei (^{23}Al and ^{27}P) with that of stable nuclei (^{27}Al and ^{31}P).

Figure 3: The neutron (blue curves), proton (brown curves), and matter (red curves) show densities of ^{23}Al and ^{27}P, respectively. The proton diffuseness is also larger than the neutron diffuseness in these nuclei. There is a large density difference between the proton and neutron in ^{23}Al and ^{27}P. The usual performance of the halo nucleus (i.e., the long tail) is apparent in the proton density distributions (brown curves), as indicated by these figures. For ^{23}Al and ^{27}P, the difference between the *rms* radii of the proton and the neutron is (r_p - r_n = 0.52613, 0.65066 *fm*). This difference is also supported by the halo structure of these alien cores.

It is seen from the Figure 4 a plotted for the elastic form factor versus q (in fm^{-1}) for ^{23}Al and ^{27}P calculated with PWBA. The blue solid curve represents the form factor for 2BCDD's with ($F_{fs}\neq0$, $F_{cm}\neq0$) and oscillator size parameter (b_m =1.87 *fm* for ^{23}Al and b_m=1.912 *fm* for ^{27}P), the red curve represents the form factor for 2BCDD's with correlation and oscillator size parameter (b_m =1.87 *fm* for ^{23}Al and b_m=1.912 *fm* for ^{27}P), (F_{fs} = 0, F_{cm} = 0) i.e the finite nucleon size and the center of mass corrections doesn't take into account. The filled circle represents the experimental elastic form factors of ^{27}Al and ^{31}P [28]. The form factor is determined by the detailed properties of a single proton halo as well as the difference, which is determined by the mass number and the size parameter bm. We obtain good agreement at the momentum for q<3.6, and we note that the behavior of the theoretical results for halo nuclei (^{23}Al and ^{27}P) matches the practical results for stable nuclei (^{27}Al and ^{31}P).

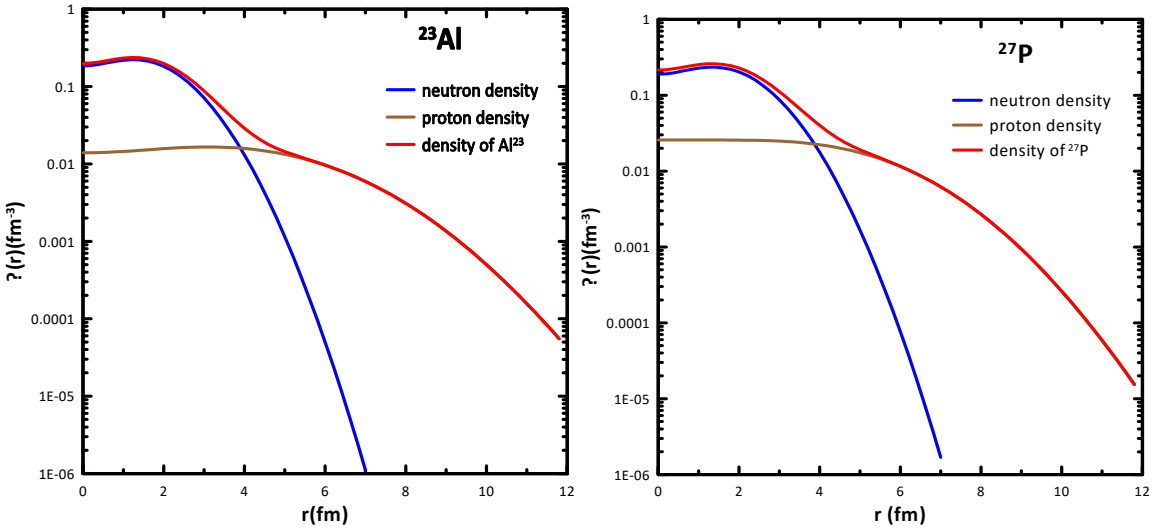

Figure 3. Comparison of proton, neutron and matter densities for ^{23}Al and ^{27}P halo

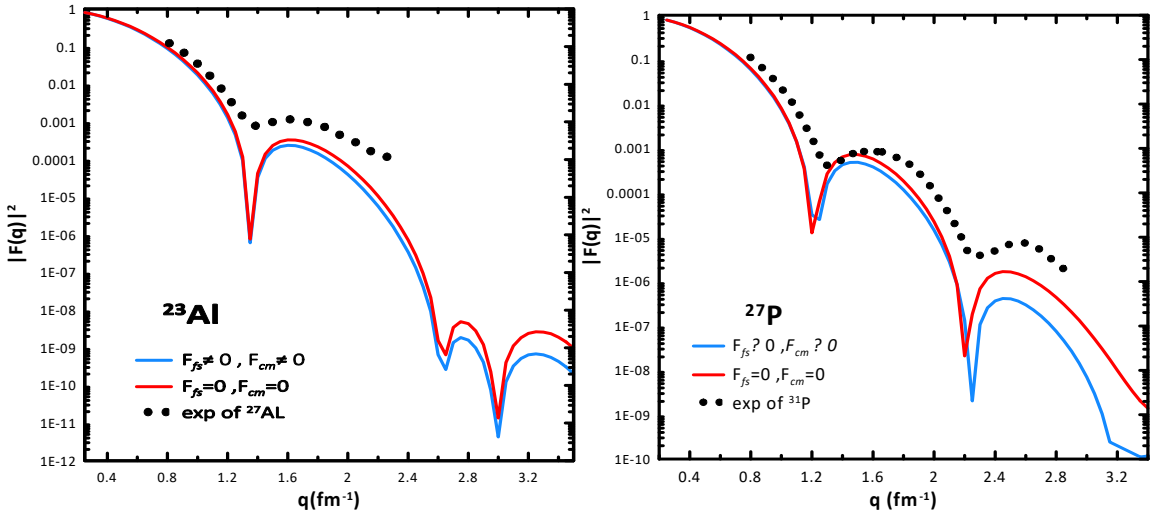

Figure 4. The form factors for ^{23}Al and ^{27}P nuclei with experimental data [28].

4. CONCLUSIONS

In this work, halo nuclei are known to have a valence of a proton, the halo of a proton occupies a $2s_{1/2}$ orbital. The measured material density of our halo nuclei showed a long-tailed behavior using the two-body nucleus density distribution framework with two different oscillator size parameters b_c and b_v with tensor force effects (Increasing its effect, the rms radii increases) and the short range (the increase its effect, the rms radii decreases), which are consistent with the experimental data. The large variation in charge form factors between unstable nuclei (^{23}Al and ^{27}P) and stable isotopes (^{27}Al and ^{31}P) is due to the same charge distribution of the protons.

ORCID IDs
Abeer A.M. Hussein, https://orcid.org/0000-0003-0068-1347; **Ghaith N. Flaiyh,** https://orcid.org/0000-0001-9918-4484

REFERENCES

[1] B.A. Brown, and P.G. Hansen, Phys. Lett. B, **381**, 391, (1996). https://doi.org/10.1016/0370-2693(96)00634-X
[2] P.G. Hansen, and B. Jonson, Europhys. Lett. **4**, 409 (1987). https://doi.org/10.1209/0295-5075/4/4/005
[3] J. Meng, and P. Ring, Phys. Rev. Lett. **80**, 460 (1998). https://doi.org/10.1103/PhysRevLett.80.460
[4] I. Tanihata, T. Kobayashi, O. Yamakawa, S. Shimoura, K. Ekuni, K. Sugimoto, N. Takahashi, et al., Phys. Lett. B, **206**, 592, (1988). https://doi.org/10.1016/0370-2693(88)90702-2
[5] I.J. Thompson, S. Al-khalili, J.A. Tostevin, and J.M. Bang, Phys. Rev. C, **47**, 1364 (1993). https://doi.org/10.1103/PhysRevC.47.R1364
[6] W. Schwab et al., Z. Phys. A, **350**, 283 (1995). https://doi.org/10.1007/BF01291183
[7] A. Ozawa, et al., Phys. Lett. B, **334**, 18 (1994). https://doi.org/10.1016/0370-2693(94)90585-1
[8] E. Ryberg, C. Forss´ena, H.-W. Hammer, and L. Platter, "Range corrections in proton halo nuclei", Nucl. Phys. **367**, 13 (2016). https://doi.org/10.1016/j.aop.2016.01.008
[9] F. Dellagiacoma, G. Orlandiniand, and M. Traini, "Dynamical correlations in finite nuclei: A simple method to study tensor effects", Nucl. Phys. A, **393**, 1, 95-108 (1983).
[10] J. Da Providencia, and C. M. Shakin, "Some aspects of short-range correlation in nuclei", Ann. Phys. **30**(1), 95-118 (1964).
[11] A. Malecki and P. Picchi, "Elastic electron scattering from4He", Phys. Rev. Lett. **21**(19), 1395-1398 (1968). https://doi.org/10.1103/PhysRevLett.21.1395
[12] L.F. Sultan, and A.N. Abdullah, "Study of the Proton Halo Structure of Nuclei ^{23}Al and ^{27}P Using the Binary Cluster Model", Iraqi Journal of Physics, **19**(48), 21 (2021). https://ijp.uobaghdad.edu.iq/index.php/physics/article/view/581
[13] R.I. Noori, and A.R. Ridha," Density Distributions and Elastic Electron Scattering Form Factors of Proton-rich ^{8}B, ^{17} F, ^{17}Ne, ^{23}Al and ^{27}P Nuclei", Iraqi Journal of Science, **60**(6), 1286-1296 (2019). https://doi.org/10.24996/ijs.2019.60.6.12
[14] M.T. Yaseen, and A.M. Ali, "Charge Density Distributions, Momentum Density Distribution, and Elastic Form Factors of Exotic One- And Two-Proton Halo Nuclei", Journal of Critical Reviews, **7**(15), (2020). https://www.jcreview.com/admin/Uploads/Files/61f278fc50d2d4.61077221.pdf
[15] A.K. Hamoudi, G.N. Flaiyh, and A.N. Abdullah, Iraqi Journal of Science, **56**(1A), 147 (2015). https://www.iasj.net/iasj/download/e5ff2f1a46127a57
[16] A.N. Antonov, P.E. Hodgson, and I.Z. Petkov, *Nucleon Momentum and Density Distributions in Nuclei*, (Clarendon Press, Oxford, 19880, pp. 97-102.
[17] S. Gartenhaus, and C. Schwartz, Phys. Rev. **108**(2), 482 (1957). https://doi.org/10.1103/PhysRev.108.482
[18] J. Fiasi, A. Hamoudi, J.M. Irvine, and F. Yazici, J. Phys. G: Nucl. Phys. **14**, 27 (1988). https://doi.org/10.1088/0305-4616/14/10/002
[19] A.N. Abdullah, Int. J. Mod. Phys. E, **29**, 2050015 (2020). https://doi.org/10.1142/S0218301320500159
[20] T.T.S. Kuo, and G.E. Brown, Nucl. Phys. A, **85**, 40-86 (1966). https://doi.org/10.1016/0029-5582(66)90131-3
[21] A.N. Antonov, M.K. Gaidarov, D.N. Kadrev, P.E. Hodgson, and E.M.D. Guerr, Int. J. Mod. Phys. E, **13**, 759 (2004). https://doi.org/10.1142/S0218301304002430
[22] T. de Forest, Jr., and J.D. Walecka, "Electron scattering and nuclear structure", Adv. Phys. **15**(1), 1 (1966). https://doi.org/10.1080/00018736600101254
[23] J.D. Walecka, *Electron Scattering for Nuclear and Nucleon Structure*, (Cambridge University Press, Cambridge, 2001), pp. 14-16.
[24] G. Audi, F.G. Kondev, M. Wang, W.J. Huang, and S. Naimi, Chin. Phys. C, **41**, 030001 (2017). http://dx.doi.org/10.1088/1674-1137/41/3/030001
[25] H.Y. Zhang, W.Q. Shen, Z.Z. Ren, Y.G. Ma, W.Z. Jiang, Z.Y. Zhu, X.Z. Cai, et al. Nuclear Physics A, **707**, 303–324 (2002). https://doi.org/10.1016/S0375-9474(02)01007-2
[26] Y.L. Zhao, Z.Y. Ma, B.Q. Chen, and W.Q. Shen, "Halo structure of nucleus ^{23}Al", Chinese Physics Letters, **20**(1), 53-55 (2003). http://dx.doi.org/10.1088/0256-307X/20/1/316
[27] A.N. Abdullah, "Systematic Study of the Nuclear Structure for Some Exotic Nuclei Using Skyrme–Hartree–Fock Method", Iran. J. Sci. Technol. Trans. Sci. **44**, 283 (2020). https://doi.org/10.1007/s40995-019-00799-x
[28] H. De Vries, and C.W. Jager, "Nuclear charge-density-distribution parameters from elastic electron scattering", Atomic Data and Nuclear Data Tables, **36**(3), 495-536 (1987). https://doi.org/10.1016/0092-640X(87)90013-1

ТЕОРЕТИЧНЕ ДОСЛІДЖЕННЯ СТРУКТУРИ ПРОТОННОГО ГАЛО ТА ФОРМ-ФАКТОРА ПРУЖНОГО РОЗСІЯННЯ ЕЛЕКТРОНІВ ДЛЯ ЯДЕР ^{23}Al ТА ^{27}P ЗА ВИКОРИСТАННЯ ПОВНИХ КОРЕЛЯЦІЙНИХ ФУНКЦІЙ (ТЕНЗОРНА СИЛА І КОРОТКОДІЯ)

Абір А.М. Хусейн, Гейт Н. Флей
Факультет фізики, Науковий коледж, Багдадський університет, Багдад, Ірак

Дослідження форм-факторів ядер, багатих на протони, середньоквадратичного радіуса (середньоквадратичного значення) і розподілу ядерної щільності є центром цієї роботи для ядер (^{23}Al і ^{27}P), використовується два розподіли щільності заряду (2BCDD). З ефектами сильної тензорної сили та короткодії функція розподілу нуклонів двох осцилюючих гармонійних частинок у двочастотній моделі оболонки працює з двома різними параметрами: bc для внутрішніх (ядерних) орбіт і bv для зовнішніх (гало) орбіталей. Ця робота продемонструвала існування ядер протонного гало для ядер (^{23}Al і ^{27}P) в оболонці (2s1/2), а обчислені розподіли густини протонів, нейтронів і речовини для цих ядер показали довгий хвіст продуктивності. Використовуючи борнівське наближення плоскої хвилі, було розраховано пружний форм-фактор розсіювання електрона від чужорідного ядра, цей форм-фактор залежить від різниці в розподілі густини протонів останнього протона в ядрі. Для розрахунку нейтронів, протонів, щільності речовини, форм-фактора пружного розсіювання електронів і середньоквадратичних радіусів використовувалася програма PowerStation Fortran 95. Розраховані результати для цих екзотичних ядер добре узгоджуються з експериментальними даними.

Ключові слова: *екзотичні ядра; форм-фактор; багатопротонні ядра; середньоквадратичні радіуси*